The Canadian Mineralogist
Vol. 37, pp. 997-1006 (1999)

THE STRUCTURAL FORMULA OF TALC FROM THE TRIMOUNS DEPOSIT, PYRENÉES, FRANCE

FRANÇOIS MARTIN[§] AND PIERRE MICOUD

Laboratoire de Minéralogie, Université Paul Sabatier – Toulouse III, UMR 5563 du CNRS, 39, Allées Jules Guesde, F-31000 Toulouse, France

LUC DELMOTTE, CLAIRE MARICHAL AND RONAN LE DRED

Laboratoire Matériaux Minéraux, URA 0428, CNRS, Ecole Nationale Supérieure de Chimie de Mulhouse, 3, rue Alfred Werner, F-68093 Mulhouse Cedex, France

PHILIPPE DE PARSEVAL

Laboratoire de Minéralogie, Université Paul Sabatier – Toulouse III, UMR 5563 du CNRS, 39, Allées Jules Guesde, F-31000 Toulouse, France

ALAIN MARI

Laboratoire de Chimie de Coordination, CNRS, 205 Route de Narbonne, F-31077 Toulouse Cedex, France

JEAN-POL FORTUNÉ, STEFANO SALVI AND DIDIER BÉZIAT

Laboratoire de Minéralogie, Université Paul Sabatier – Toulouse III, UMR 5563 du CNRS, 39, Allées Jules Guesde, F-31000 Toulouse, France

OLIVIER GRAUBY

Centre de Recherche de la Modélisation et de la Croissance Cristalline, CNRS, Campus de Luminy, Case 913, F-13288 Marseille Cedex 9, France

JOCELYNE FERRET

Talc de Luzenac S.A., BP 1162, F-31036 Toulouse Cedex, France

Abstract

A sample of talc (T111) from the Trimouns deposit, in the Pyrénées, France, was studied by various spectroscopic methods (FTIR, NMR, EPR and Mössbauer), as well as HRTEM and X-ray diffraction, in order to investigate the extent of minor substitutions in the tetrahedral and octahedral sites. Substitutions cause a deficiency in tetrahedral charge, compensated by an excess in octahedral charge, ensuring an electroneutrality of the structure. The charge deficiency on the layer of tetrahedra explains the active interaction between talc (used as filler) and polymer.

Keywords: talc, tetrahedral site, octahedral site, substitutions, spectroscopy, charge deficiency, polymer, Trimouns, Pyrénées.

Sommaire

Un échantillon de talc (T111) provenant du gisement de Trimouns (Pyrénées, France) a été étudié en détail à l'aide des spectroscopies FTIR, NMR, EPR et Mössbauer, du microscope électronique à transmission et de la diffraction des rayons X afin de quantifier les faibles taux de substitution dans les sites tétraédriques et octaédriques. Les résultats montrent que le feuillet du talc T111 est électriquement neutre, avec un déficit de charge tétraédrique compensé par un excès de charge octaédrique, ceci étant dû aux nombreuses substitutions. Le déficit local de surface de la couche tétraédrique peut expliquer les interactions actives entre le talc, utilisé comme charge minérale, et les polymères.

Mots-clés: talc, site tetraédrique, site octaédrique, substitutions, spectroscopies, déficit de charge, polymères, Trimouns, Pyrénées.

§ *E-mail address*: martinf@cict.fr

Introduction

Talc ore is used in paper coating, and its properties make it useful in the paint, ceramics, and polymer industries. In the automotive industry, talc is added to polymers to stabilize and harden parts of automobiles like fenders, dashboard, and steering wheel. However, various problems appear with these materials, notably an undesirable coloring in ceramics and polymers (blush), and variable behavior in polymer applications. To improve the use of various types of talc in specific industrial applications, it is necessary to take into account the physical and chemical properties of the talc. In this paper, we characterize the chemical composition of a sample of pure talc (T111) from the Trimouns deposit, the largest of the world. The results of this study improve our knowledge of the extent of substitutions in talc from this deposit by detailed characterization of element distributions (Fe^{2+}, Fe^{3+}, Al, Mn^{2+}, F), using various spectroscopic techniques.

Background Information

Most samples of talc (2:1 layer silicate) typically have a near-end-member composition [$Mg_3Si_4O_{10}(OH)_2$], and in many cases no interlayer exists because the 2:1 layer is electrostatically neutral. However, major amounts of Fe, minor amounts of Al and F, and traces of Mn, Ti, Cr, Ni, Na and K have been reported in talc (Heller-Kallai & Rozenson 1981, Noack *et al.* 1986, Abercrombie *et al.* 1987, Aramu *et al.* 1989, Coey *et al.* 1991, de Parseval *et al.* 1991, 1993). These authors documented the various potential substitutions in the tetrahedral (Si replaced by Fe^{3+}, Al) and octahedral sites (Mg replaced by Fe^{2+}, Fe^{3+}, Al), but did not establish charge balance of these natural samples of talc.

Geological Context

The Trimouns talc and chlorite deposit is located in the French Pyrénées, 100 km south of Toulouse, at an altitude of 1,700 m. It occurs along the eastern side of the Hercynian Saint Barthélémy Massif of gneissic rocks. The mode of formation of the talc and chlorite in the deposit is now well established (Fortuné *et al.* 1980, Moine *et al.* 1982, 1989, de Parseval *et al.* 1993). These minerals originated by hydrothermal alteration of wallrock in a zone of intense shearing between the Saint Barthélémy dome and the low-grade Paleozoic metamorphic cover. Dolostones of the Paleozoic cover were transformed to talc, whereas siliceous and aluminous rocks (mica-bearing schists and granitic pegmatites) were completely transformed to chlorite-dominant ore characterized by well-defined metasomatic zones. The transformation of dolostone to talc involved addition of Si, leaching of Ca, and loss of CO_2 during the alteration. The talc ore exhibits facies that vary in color from pure white to grey and to black, the latter being principally due to inclusions of graphite. The total iron content of the talc ore is about $0.6 \pm 0.2\%$ Fe_2O_3, but no separate iron-bearing phase has been detected.

Analytical Methods

Chemical analyses

Whole-rock analysis were performed by Inductively Coupled Plasma (ICP) at the CRPG in Nancy. The chemical composition of the talc was determined using a Cameca SX–50 electron microprobe at the Université Paul Sabatier in Toulouse. Operating conditions were 15 kV and 10 nA, and natural and synthetic standards were used.

X-ray diffraction (XRD)

The talc from the Trimouns deposit was analyzed by X-ray diffraction (XRD). The spectra were collected in reflection mode using a Philips PW1130 diffractometer with Ni-filtered Cu$K\alpha$ radiation (30 kV, 30 mA). The spectra were recorded for 3.5 s per step of 0.0005° from 2° to 80° (θ). With this approach, the limit of detection of a phase was established at 0.5%.

Fourier transform infrared spectroscopy (FTIR)

Fourier transform infrared (FTIR) spectra were recorded in transmission mode in the 4000–400 cm^{-1} range on a Nicolet 510 FTIR spectrometer. The pellets were prepared by mixing 4 mg sample with 300 mg KBr.

^{57}Fe Mössbauer spectroscopy

A ^{57}Fe Mössbauer absorption spectrum was recorded over the range ±4 mm/s with 512 channels in the Laboratoire de Chimie de Coordination in Toulouse. The Mössbauer spectrometer is composed of a compact detector γ-system for high count-rates and a conventional constant-acceleration Mössbauer device (WISSEL). A ^{57}Co (in Rh) source with nominal activity of 50 mCi was used. Powders were finely ground under acetone (to minimize possible oxidation of Fe) and placed in a plexiglass sample holder. The spectra were obtained at room temperature, 80 K and 4 K, and, were recorded with a Canberra multichannel analyzer, coupled to a computer. The isomer shift was recorded with respect to α-Fe metal. As advocated by Rancourt *et al.* (1993), the absorber thickness of the talc sample was approximated to that of micas in the phlogopite–annite series; in particular, phlogopite has a Fe content similar to that of talc T111. This was done to minimize the width of the absorption lines in the spectra. The values are around 200 mg of mineral per cm^2. Lorentzian line-shapes were assumed for deconvolutions, based on least-squares fitting procedures. The ψ^2 and misfit values were used to measure the goodness of the computer fit.

Electron paramagnetic resonance (EPR) spectroscopy

All EPR spectra were recorded at room temperature with a Bruker ESP–300e spectrometer operating at X-band frequency (9 GHz). A mercury lamp was used as UV radiation source (200 W), irradiating the ESR cavity through the medium of a quartz optical fiber. This procedure allowed us to follow the evolution of the ESR spectrum of the sample during the UV irradiation.

Nuclear magnetic resonance (NMR) spectroscopy

The solid-state nuclear magnetic resonance experiments were performed as follows: ^{29}Si NMR measurements were carried out on a Bruker MSL–30 spectrometer operated at $B_0 = 7.1$ T ($\nu_0 = 59.63$ MHz) with B_0 the magnetic field. The NMR spectra of ^{27}Al and ^{19}F were recorded on a Bruker DSX–400 spectrometer operating at $B_0 = 9.4$ T ($\nu_0 = 104.263$ and 376.49 MHz, respectively). Single-pulse magic-angle spinning (MAS) spectra were obtained using a Bruker MAS probe with a 7 mm ZrO_2 rotor for the ^{29}Si experiment and a 4 mm rotor for the ^{27}Al and ^{19}F experiments. Acquisitions parameters are summarized in Table 1. Chemical shifts of ^{29}Si, ^{27}Al and ^{19}F were externally compared to TMS (tetramethylsilane), $CFCl_3$ (trichlorofluoromethane), and aqueous $Al(H_2O)_6^{3+}$, respectively. The deconvolutions were carried out with WINFIT (Bruker program) by using the Gaussian model.

TABLE 1. NMR ACQUISITION PARAMETERS FOR TALC T111

Nucleus	^{29}Si	^{19}F	^{27}Al
Spinning speed (kHz)	4	12	10
Pulse length (flip angle)	3.25 μs (π/4)	3.6 μs (π/2)	1 μs (π/12)
Recycle delay	2 mn	10 s	1 s

High-resolution transmission electron microscopy (HRTEM)

For observations using high-resolution transmission electron microscopy, slices of the specimen containing optically selected areas were removed from thin sections and ion-thinned with an argon beam following the procedure described by Amouric & Parron (1985). Electron microscopy was performed at Centre de Recherche de la Modélisation et de la Croissance Cristalline (CRMC^2, Marseille, France) with a JEOL–2000 FX instrument, equipped with an energy-dispersion X-ray spectrometer for chemical micro-analysis. The microscope was operated at 200 kV for HRTEM imaging, electron diffraction and micro-analysis (Baronnet *et al.* 1993).

TABLE 2. CHEMICAL COMPOSITION OF TALC T111

	Electron Microprobe*	ICP		Electron Microprobe*	ICP
SiO_2	62.92	61.67	K_2O	0.02	Tr
Al_2O_3	0.09	0.19	TiO_2		Tr
$Fe_2O_{3(T)}$	0.59	0.68	P_2O_5		0.11
MnO	0.02	Tr	F	0.23	
MgO	31.11	31.52	$S_{(T)}$		Tr
CaO	0.02	0.02	H_2O	4.60	4.84
Na_2O	0.01	Tr	Total	99.61	99.03

* Results of electron-microprobe analyses based on 10 points.
ICP : Inductively Coupled Plasma

RESULTS

Chemical composition

The talc sample was selected from a vein of pure talc; it is representative of ore in the Trimouns deposit, and was carefully hand-picked. Its chemical composition (Table 2) indicates a virtually monomineralic sample, with no accessory minerals and no Fe-bearing minerals, such as sulfides.

XRD

The powder-diffraction pattern is characteristic of pure talc; no other phases (> 0.5%) were detected (Fig. 1). The powder pattern exhibits sharp *hkl* reflections, indicative of a well-ordered three-dimensional structure, with coherency of domains on the scale of 1100 Å along the c^* axis (Fig. 1).

FTIR

FTIR spectroscopy is a very sensitive probe of the possible talc–chlorite association, especially in the OH-stretching region; three vibration bands are expected for chlorite, and only one for talc. According to Farmer (1958), Vedder (1964), Farmer & Russell (1967), Farmer *et al.* (1968), Ishii *et al.* (1967) and Grauby *et al.* (1991), the vibrations of pure talc are as follows: 1) ν_1 and ν_2 for Si–O stretching vibrations at 1040 and 687 cm^{-1}, respectively, 2) ν_3 for Si–O–Si stretching vibrations at 1014 cm^{-1}, 3) ν_4 for Si–O–Si bending vibrations around 460 cm^{-1}, 4) ν_5 for *M*–OH ⊥ (octahedral

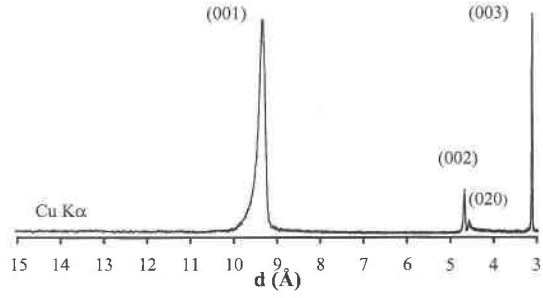

FIG. 1. X-ray-diffraction pattern of talc T111.

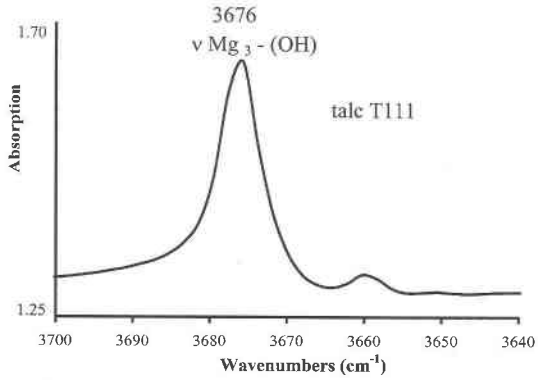

FIG. 2. Infrared spectra of talc T111 in the stretching region.

oxygen atoms and hydroxyl groups, vibrations of octahedra moving in opposition to octahedrally coordinated cations) at 535 cm^{-1}, 5) ν_6 for *M*–OH ⊥ (octahedrally coordinated cations moving in phase with their adjacent sheets of oxygen atoms, relative to sheets of silicon and surface oxygen atoms) at 259 cm^{-1}, 6) ν_7 for trans (OH) // (translatory vibration of hydroxyl groups, out of phase with the other oxygen atoms in this sheet) at 465 cm^{-1}, and 7) δOH for OH librations at 669 cm^{-1}.

The OH-stretching region (3800–2500 cm^{-1})

The vibrational spectrum (Fig. 2) corresponds to that of pure talc and is very simple in this wavenumber range. It displays only one sharp band located at 3676 cm^{-1}, indicating an extremely regular environment around the hydroxyl group. Another vibrational band exists (not attributed in past investigations), located at 3660 cm^{-1}. It is invariably observed in pure talc, with an intensity depending on the extent of substitutions in the octahedral sites (F. Martin and S. Petit, in prep.). This band is not observed in chlorite-group minerals.

The 1200–300 cm^{-1} region

In this complex region, the spectrum shows well-defined absorption bands characteristic of pure talc (Fig. 3), with ν_2 at 668 cm^{-1} and δOH at 685 cm^{-1}. No vibration bands of chlorite are detected.

HRTEM

Figures 4a and 4b show the electron-diffraction pattern and the lattice image of massive talc T111 from the Trimouns deposit. The diffraction pattern corresponds to the one-layer triclinic structure, with the *c** axis perpendicular to the electron-diffraction image. The lattice image consists of a single set of lattice fringes of pure talc that is well correlated with the diffraction pattern. The stacking faults observed were induced during sample preparation.

Mössbauer spectra

Table 3 lists the possible site-occupancies in talc and a listing of the δ and Δ values determined on various minerals by Rancourt *et al.* (1992, 1994b) and Rancourt (1994b), and taking into account the quadrupole splitting distributions (Rancourt 1994a).

Ideal talc is conventionally represented by the formula $Mg_3Si_4O_{10}(OH)_2$, with Fe replacing Mg in the octahedral sites. Mössbauer spectra of talc have been previously reported (Coey 1980, Blaauw *et al.* 1980, Heller-Kallai & Rozenson 1981, Noack *et al.* 1986,

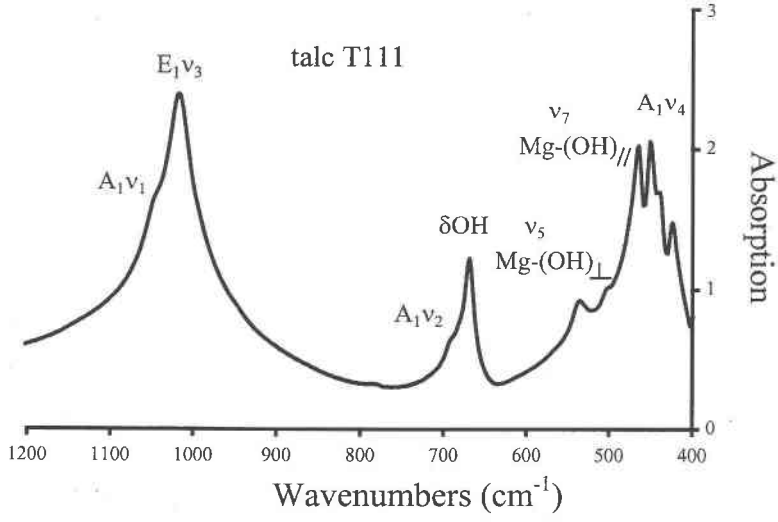

FIG. 3. Infrared spectra of talc T111 in the 1200–400 cm^{-1} region.

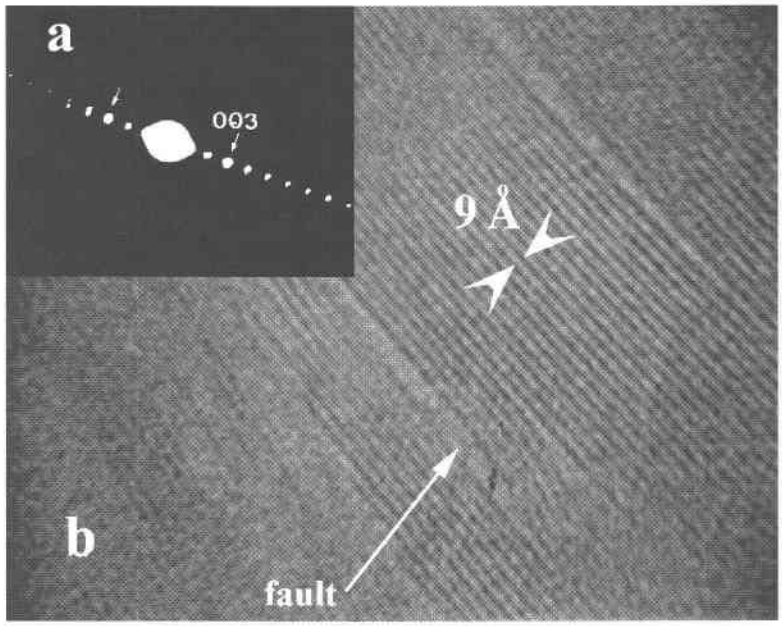

FIG. 4. a. Electron-diffraction pattern of massive talc T111. b. Lattice image of massive talc T111. High-resolution transmission electron microscopy.

Aramu *et al.* 1989, Coey *et al.* 1991). These authors have proposed a single doublet for octahedrally coordinated Fe^{2+}. Recent studies (Rancourt *et al.* 1992, 1993, 1994b, Rancourt (1994a, b) have demonstrated that paramagnetic state Mössbauer spectroscopy of 2:1 layer silicates cannot resolve the octahedrally coordinated Fe^{2+} in *cis* (*M*2) and *trans* (*M*1) sites. Mössbauer studies of these materials can nevertheless indicate the overall proportion and the coordination of Fe^{2+} and Fe^{3+} (Table 3).

The spectrum of talc T111 at room temperature (Fig. 5a) is similar to spectra obtained for annite by Rancourt *et al.* (1994). It shows a difference in intensity between the two absorption bands, and an important shoulder on the side of the peak located at –0.5 mm/s.

TABLE 3. DIFFERENT SITE-OCCUPANCIES OF IRON IN TALC T111 AND THE PHLOGOPITE-ANNITE SERIES AND MÖSSBAUER PARAMETERS USING THE QSD MODEL

Site occupancies	Talc	Phlogopite*		Annite*	
		δ	Δ	δ	Δ
$^{[4]}Fe^{2+}$	-				
$^{[4]}Fe^{3+}$	+	0.193	0.404	0.217	0.328
					2.600
$^{[6]}Fe^{2+}$	+	1.146	2.666	1.087	2.345
			2.517		2.113
$^{[6]}Fe^{3+}$	+	0.435	1.000	0.411	1.085

- not present, + present
* Mössbauer parameters of phlogopite and annite (Rancourt *et al.* 1994c)

The deconvolution in Lorentzian doublets (Fig. 5b) is made with two components: one according to Fe^{2+} in octahedral sites, with a large quadrupole splitting (Table 4), and one inside the first absorption band, with a small quadrupole splitting and a low isomer shift (Table 4), attributed to Fe^{3+} in the tetrahedral site (Dyar & Burns 1986, Rancourt *et al.* 1992, 1993). No orientation effects are present in spectra (the electric field gradients of $^{[6]}Fe^{3+}$, $^{[4]}Fe^{3+}$ and $^{[6]}Fe^{2+}$ have different orientations).

The same sample was recorded at 80 K (Fig. 6a) to benefit from the second-order Doppler effect. The deconvolution (Fig. 6b) is made with various contributions corresponding to those obtained at room temperature, and with two doublets whose Mössbauer parameters correspond to Fe^{3+} in octahedral sites (Blaauw *et al.* 1980, Dyar & Burns 1986, Rancourt *et al.* 1992, Dyar 1993, Rancourt 1993). The iron is distributed (except for Fe^{2+} in the tetrahedral site) in both sites, Fe^{2+} being the predominant form (68%), indicative of the redox conditions during the formation of talc.

In Table 4, we report Mössbauer parameters for talc T111 at 80 K. The parameters of tetrahedrally coordinated Fe^{3+} are very close to those encountered in micas (Dyar & Burns 1986, Dyar 1987, 1993, Rancourt *et al.* 1992, Rancourt 1993). The same conclusions are possible for the other Mössbauer parameters, with large quadrupole split for Fe^{2+} in octahedral sites due to the temperature at which the spectrum was recorded.

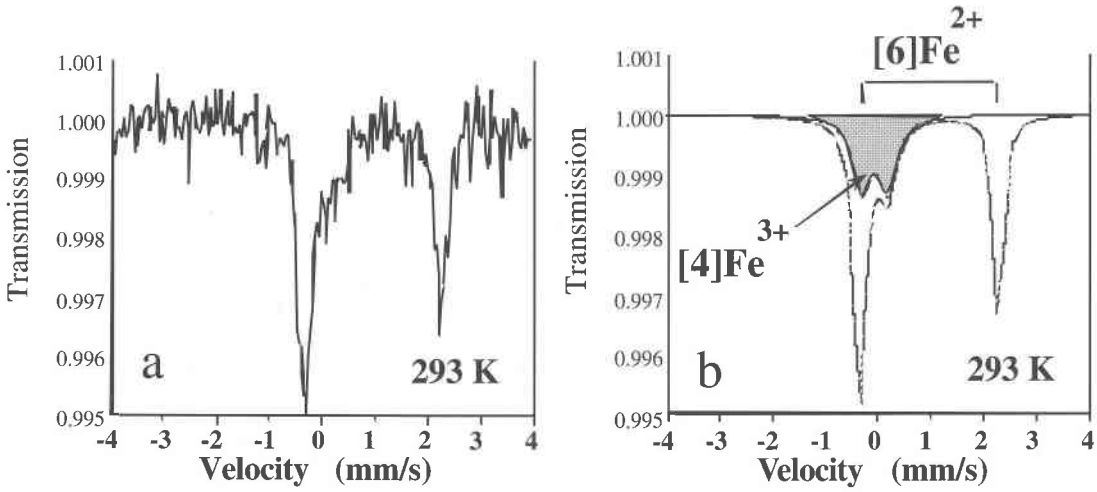

FIG. 5. a. Room-temperature experimental Mössbauer spectrum of talc T111. b. Calculated spectrum of talc T111 at room temperature.

Solid-state NMR

The ^{19}F MAS–NMR spectrum of talc T111 exhibits one resonance at –176.2 ppm (Fig. 7), indicating that only one site is present in the structure (Huve *et al.* 1992). This signal has already been observed for trioctahedral 2 :1 layer silicate and is attributed to F atoms bonded to three atoms of Mg (Mg–Mg–Mg configuration).

The ^{29}Si isotropic shift is strongly influenced by the chemical environment of the silicon nucleus and is highly correlated with the degree of polymerization of the SiO_4 tetrahedra (Lippmaa *et al.* 1980, 1981, Mägi *et al.* 1984, Kirkpatrick 1988). Furthermore, in layer silicates, characteristic high-field shifts are observed with a decreasing number of next-near-neighbor Al atoms (Kinsey *et al.* 1985). The ^{29}Si MAS–NMR spectrum of talc T111 shows an asymmetrical peak at –96.8 ppm, attributed to Q^3 species, characteristic of clay minerals. The shoulder observed at low field can be explained by increasing incorporation of Al atoms.

It is well known that ^{27}Al MAS–NMR spectroscopy is a powerful tool with which to distinguish readily and unambiguously between four- and six-fold-coordinated aluminum atoms because of well-separated shifts in range (Barron *et al.* 1985, Herrero *et al.* 1985a, b). For the quantitative aspect of ^{27}Al NMR, selective conditions of excitation are induced by taking very short du-

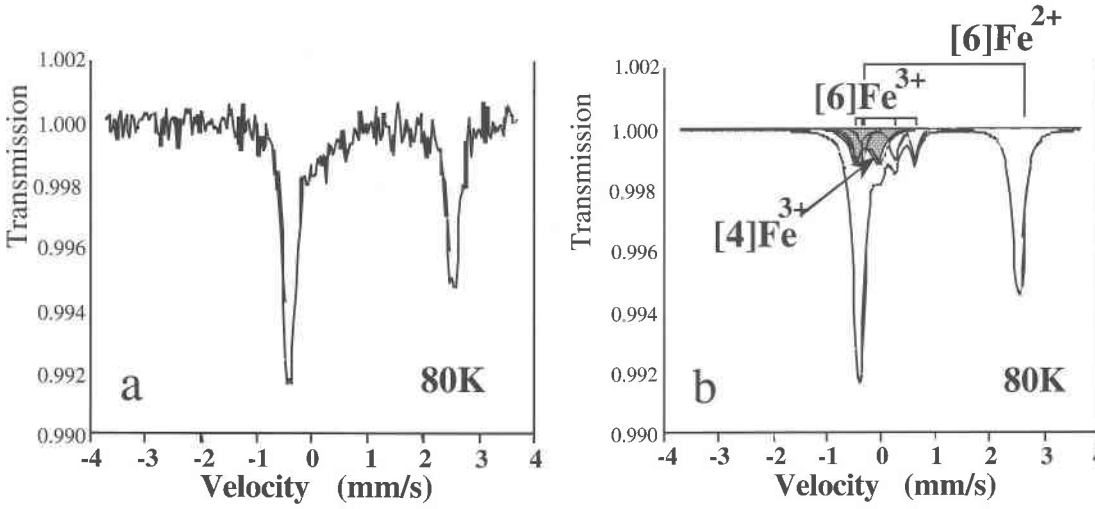

FIG. 6. a. Experimental Mössbauer spectrum of talc T111 at 80 K. b. Calculated spectrum of talc T111 at 80 K.

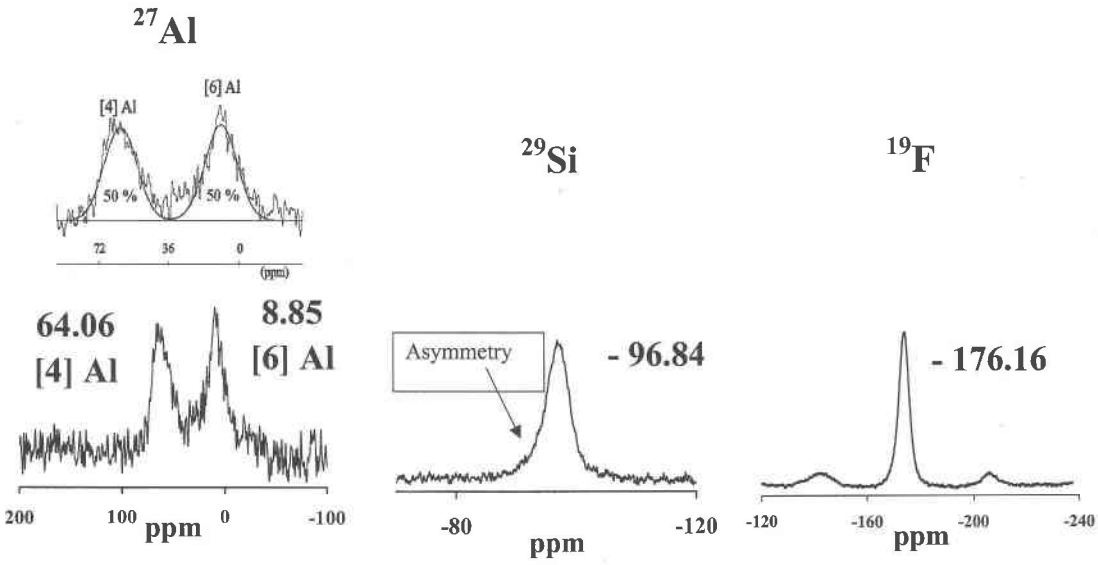

FIG. 7. Si, F, and Al MAS NMR spectra of talc T111.

rations of impulse (0.7 μs) with very-weak-field radio-frequencies (flip angle = π/12). Under these conditions, all the types of aluminum in the sample are excited in an equivalent way. The ^{27}Al MAS–NMR spectrum of talc T111 shows two resonances at 8.9 and 64.1 ppm, corresponding to Al in octahedral and tetrahedral sites, respectively. The integrated area under each NMR peak (Fig. 7) show that both $^{[4]}$Al and $^{[6]}$Al are present in roughly equivalent amounts.

Electron paramagnetic resonance spectroscopy

Electron paramagnetic resonance spectroscopy is used to detect unpaired electrons, such as in Fe^{3+} and Mn^{2+}, and to characterize their chemical environments. The EPR spectrum of talc T111 at room temperature (Fig. 8) shows a sextet at g = 2.0 characteristic of Mn^{2+} in the octahedral site and a small signal around g = 4 (Goodman & Hall 1994). But at a low temperature (4 K), a well-resolved spectrum is obtained (Fig. 8), with two distinct signals, one located at g = 4.3, characteristic of Fe^{3+} in the tetrahedral or octahedral site, and one located at g = 2, which is assigned to Mn^{2+} in the octahedral site. A possible assignment of Fe^{3+} in the tetrahedral or octahedral site is indicated by modeling the EPR powder spectra using numerical diagonalization of the spin hamiltonian (Morin & Bonnin 1999). Under UV radiation and aggressive treatments with water, no evolution in ESR spectra is evident. This observation indicates that the Fe^{3+} content reveals the redox conditions during the formation of the talc.

TABLE 4. MÖSSBAUER PARAMETERS OF TALC T111 AT ROOM TEMPERATURE AND 4 K

	Fe^{2+}				Fe^{3+}				
	δ* (mm/s)	Δ (mm/s)	%	Site	δ* (mm/s)	Δ (mm/s)	%	Site	$\frac{Fe^{2+}}{(Fe^{2+}+Fe^{3+})}$
					-0.08	0.40	14.7	[4]	
talc T111	1.15	2.93	67.5	[6]	0.40	0.71	17.8	[6]	67.5
	1.24	2.96			0.30	0.95			

* δ value relative to Fe-metal

SUMMARY OF SPECTROSCOPIC INVESTIGATIONS AND ELECTRON-MICROPROBE DATA

XRD, HRTEM and FTIR investigations show that talc sample T111 is a pure phase. Small amounts of Fe, Al, Mn, and F are incorporated into the structure. According to Mössbauer, NMR and EPR spectrocopies, it is possible to determine site assignments for these elements (Table 5).

The structural formula obtained by these various techniques and based on results of analyses of talc T111 with an electron microprobe (taking into account the standard deviation of each element), according the electroneutrality of the structure and on the basis of (O + OH + F) = 12, is:

$$[Mg_{2.978}Fe^{2+}_{0.019}Mn^{2+}_{0.001}Fe^{3+}_{0.005}Al_{0.007}]_{\Sigma 3}$$
$$[Si_{3.984}Fe^{3+}_{0.004}Al_{0.007}]_{\Sigma 4}O_{10}(OH)_{1.952}F_{0.048}$$

In the tetrahedral sheet, a charge deficit appears: 0.011. In the octahedral sheet, there is a charge excess of 0.012. However, it seems clear that a deficiency in tetrahedral charges due to the replacement of Si by Fe^{3+} and Al is compensated by an excess in octahedral

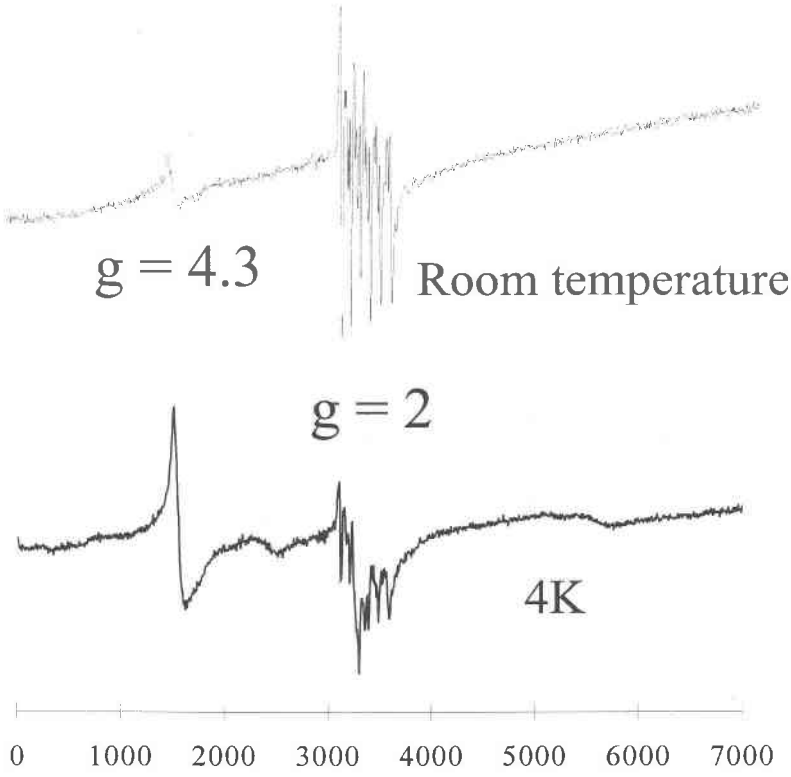

FIG. 8. ESR spectra of talc T111 at room temperature and 4 K.

charges generated by the replacement of Mg by trivalent cations Fe and Al.

DISCUSSION AND CONCLUSIONS

The XRD, FTIR and HRTEM data obtained on a carefully hand-picked sample of talc indicate that it is monomineralic and does not contain any Fe-bearing phases such as sulfides. Using appropriate spectroscopic techniques, the locations of minor elements can be determined. The resulting spectral signatures are characteristic of those obtained in similar clay minerals. On this basis, we consider all the Al, Fe, Mn, and F to belong to the structure of the talc.

TABLE 5. CONTENT AND LOCATION OF VARIOUS ELEMENTS IN TETRAHEDRAL AND OCTAHEDRAL SITES OF TALC T111

	Occupancy of sites*		Content	Normalized content	
	Fe^{2+}	Fe^{3+}		Fe^{2+}	Fe^{3+}
Fe	^{6}[67.5]	^{6}[17.8] ^{4}[14.7]	0.028	^{6}[0.019]	^{6}[0.005] [0.004]
		Al			Al
Al		^{6}[50] ^{4}[50]	0.014		^{6}[0.007] ^{4}[0.007]
	Mn^{2+}			Mn^{2+}	
Mn	^{6}[100]		0.001	^{6}[0.001]	
	F			F	
F	[100]		0.048	[0.048]	

*derived from spectroscopic investigations.
Cation contents in atoms per formula unit.

Mössbauer spectroscopy is very useful for a characterization of the distribution and valence of Fe in minerals, specially in talc. This study shows that Fe^{3+} occurs in the tetrahedral position in talc. Moreover, we report the systematic presence of $^{[4]}Fe^{3+}$ (14.7%), $^{[6]}Fe^{3+}$ (17.8%), and $^{[6]}Fe^{2+}$ (67.5%), with values that are similar to those encountered in Mössbauer spectra of annite (Rancourt *et al.* 1994a). Another major conclusion is the high $[Fe^{2+}/(Fe^{2+} + Fe^{3+})]$ value, approximately 68%, indicative of the redox conditions during the formation of talc.

The NMR results for Si, Al, and F indicate the nature of substitutions in the structure. For Si, the spectrum clearly demonstrates a Q^3 environment, characteristic of phyllosilicates. The shoulder on the peak indicates minor replacement of Si by Al or Fe (or both). For the F anion, the single sharp peak shows the existence of only one OH site being substituted, located in the large hex-

agonal cavity in rings of tetrahedra. But the major result, established here for the first time, is the location of Al in both octahedral and tetrahedral sites. The Al content of both sites is equivalent.

The EPR spectra confirm the presence of Fe^{3+} and Mn^{2+} in talc T111. The structural formula is written on the basis of spectroscopic and chemical results. The actual chemical composition of sample T111 indicates a deficiency in tetrahedral charges and an excess in octahedral charges, due to the various substitutions. The deficiency in tetrahedral charges is compensated by the excess charge on the sheet of octahedra. The major remark concerns the local deficiency on the sheet of tetrahedra. This local deficiency creates an active site on the surface of the talc. The local deficiency and the relatively high content of Fe^{2+} give a great oxidation potential to the talc.

In various industrial applications (*e.g.*, paper manufacturing, paints, ceramics, polymers), talc is used as a filler to reinforce the polymer structure. However, problems with aging and photo-oxidative degradation of polymers have been encountered. A change in color appears on the polymer surface upon exposure to solar radiation for long periods. Previous studies have shown that the presence of fillers may enhance the rate of degradation (Rabello & White 1996). To reduce these effects, TiO_2, carbon black, and HALS (Hindered Amino Light Stabilizer), for example, are added to the polymers. These additives exert a real influence, notably on the depth of the degraded layer (Rysavy & Tkadleckova 1992). There is, however, little information on the interactions among all the components present in the polymers. The degradation effects may result from charge deficiencies on surface of the fillers, and especially on the surface of talc, which may contain active sites.

The ultimate goal of this project is to understand the cause of the degradation of talc-bearing polymers, particularly with the help of spectroscopic evidence. For example, in the automotive industry, talc is added to polymers to stabilize and harden various parts of automobile bodies. We hope to understand the role of talc during degradation of polymers by natural UV irradiation. ESR and NMR spectroscopies are planned to study free radicals produced during UV irradiation. These free radicals could be the vector of various types of damage caused in filled polymer structures.

Acknowledgements

Support for this research was provided by the Société Anonyme Talc de Luzenac. We thank the anonymous reviewers and R.F. Martin for their constructive comments.

References

Abercrombie, H.J., Skippen, G.B. & Marshall, D.D. (1987): F–OH substitution in natural tremolite, talc, and phlogopite. *Contrib. Mineral. Petrol.* **97**, 305-312.

Amouric M. & Parron, C. (1985): Structure and growth mechanism of glauconite as seen by high resolution transmission electron microscopy. *Clays Clay Minerals* **33**, 473-482.

Aramu, F., Maxiav, G. & Delunas, A. (1989): Mössbauer spectroscopy of talc minerals. *Nuovo Cimento* **11D**, 891-896.

Baronnet, A., Nitsche, S. & Kang, Z.C. (1993): Layer stacking microstructures in a biotite single crystal. A combined HRTEM–AEM study. *Phase Trans.* **43**, 107-128.

Barron, P.F., Slade, P. & Frost, R.L. (1985): Ordering of aluminum in tetrahedral sites in mixed-layer 2:1 phyllosilicates by solid-state high-resolution NMR. *J. Phys. Chem.* **89**, 3880-3885.

Blaauw, C., Stroink, G. & Leiper, W. (1980): Mössbauer analysis of talc and chlorite. *J. de Phys.* **1**, 411-412.

Coey, J.M.D. (1980): Clay minerals and their transformations studied with nuclear techniques: the contribution of Mössbauer spectroscopy. *Atom. Energy Rev.* **18**, 73-124.

_____, Bakas, T. & Guggenheim, S. (1991): Mössbauer spectra of minnesotaite and ferrous talc. *Am. Mineral.* **76**, 1905-1909.

de Parseval, P., Fournes, L., Fortuné, J.-P., Moine, B. & Ferret, J. (1991): Distribution du fer dans les chlorites par spectrométrie Mössbauer (^{57}Fe): Fe^{3+} dans les chlorites du gisement de talc–chlorite de Trimouns (Pyrénées, France). *C. R. Acad. Sci. Paris* **312**, *Sér.* **II**, 1321-1326.

_____, Moine, B., Fortuné, J.P. & Ferret, J. (1993): Fluid–mineral interactions at the origin of the Trimouns talc and chlorite deposit (Pyrénées, France). *In* Current Research in Geology Applied to Ore Deposits (P. Fenoll Hach-Alí, J. Torres-Ruiz & F. Gervilla, eds.). Univ. of Granada, Granada, Spain (205-209).

Dyar, M.D. (1987): A review of Mössbauer data on trioctahedral micas: evidence for tetrahedral Fe^{3+} and cation ordering. *Am. Mineral.* **72**, 102-112.

_____ (1993): Mössbauer spectroscopy of tetrahedral Fe^{3+} in trioctahedral micas. Discussion. *Am. Mineral.* **78**, 665-668.

_____ & Burns, R.G. (1986): Mössbauer spectral study of ferruginous one-layer trioctahedral micas. *Am. Mineral.* **71**, 955-965.

Farmer, V.C. (1958): The infrared spectra of talc, saponite and hectorite. *Mineral. Mag.* **31**, 829- 845.

_____ & Russell, J.D. (1967): Infrared absorption spectrometry in clay studies. *Clays Clay Minerals* **15**, 121-142.

_____, _____ & Ahlrichs, J.L. (1968): Characterization of clay minerals by infrared spectroscopy. *Trans. 9th Int. Congr. Soil. Sci.* **3**, 101-110.

Fortuné, J.P., Gavoille, B. & Thiebaut, J. (1980): Le gisement de talc de Trimouns près de Luzenac (Ariège). *Int. Geol. Congr.* **26**, E10, 43 p.

GOODMAN, B.A. & HALL, P.L. (1994): Electron paramagnetic resonance spectroscopy. *In* Clay Mineralogy: Spectroscopic and Chemical Determinative Methods **5** (M.J. Wilson, ed.). Chapman & Hall, Aberdeen, U.K. (173-225).

GRAUBY O., PETIT S., ENGUEHARD, F., MARTIN, F. & DECARREAU A. (1991): XRD, EXAFS and FTIR octahedral cation distribution in synthetic Ni–Co kerolites. *Proc. 7th Euroclay Conf. (Dresden)* **2**, 447-452.

HELLER-KALLAI, L. & ROZENSON, I. (1981): The use of Mössbauer spectroscopy of iron in clay mineralogy. *Phys. Chem. Minerals* **7**, 223-238.

HERRERO, C.P., SANZ, J. & SERRATOSA, J.M. (1985a): Si, Al distribution in micas: analysis by high resolution ^{29}Si NMR spectroscopy. *J. Phys. C: Solid State Phys.* **18**, 13-22.

_____, _____ & _____ (1985b): Tetrahedral cation ordering in layer silicates by ^{29}Si NMR spectroscopy. *Solid State Commun.* **53**, 151-154.

HUVE, L., DELMOTTE, L., MARTIN, P., LE DRED, R., BARON, J. & SAEHR, D. (1992): ^{19}F MAS–NMR study of structural fluorine in some natural and synthetic 2:1 layer silicates. *Clays Clay Minerals* **40**, 186-191.

ISHII, M., SHIMANOUCHI, T. & NAKAHIRA, M. (1967): Far infrared absorption spectra of layer silicates. *Inorg. Chim. Acta* **1**, 387-392.

KINSEY, R.A., KIRKPATRICK, R.J., HOWER, J., SMITH, K.A. & OLDFIELD, E. (1985): High resolution aluminum-27 and silicon-29 nuclear magnetic resonance spectroscopic study of layer silicates, including clay minerals. *Am. Mineral.* **70**, 537-548.

KIRKPATRICK, R.J. (1988): MAS NMR spectroscopy of minerals and glasse. *In* Spectroscopic Methods in Mineralogy and Geology (F.C. Hawthorne, ed.). *Rev. Mineral.* **18**, 341-403.

LIPPMAA, E., MÄGI, M., SAMOSON, A., ENGELHARDT, G. & GRIMMER, A.-R. (1980): Structural studies of silicates by solid-state high-resolution ^{29}Si NMR spectroscopy. *J. Am. Chem. Soc.* **102**, 4889-4893.

_____, _____, _____, TARMAK, M. & ENGELHARDT, G. (1981): Investigation of the structure of zeolites by solid-state high-resolution ^{29}Si NMR spectroscopy. *J. Am. Chem. Soc.* **103**, 4992-4996.

MÄGI, M., LIPPMAA, E., SAMOSON, A., ENGELHARDT, G. & GRIMMER, A.-R. (1984): Solid-state high-resolution silicon-29 chemical shifts in silicates. *J. Phys. Chem.* **88**, 1518-1522.

MOINE, B., FORTUNÉ, J.P., MOREAU, P. & VIGUIER, F. (1989): Comparative mineralogy, geochemistry, and conditions of formation of two metasomatic talc and chlorite deposits: Trimouns (Pyrénées, France) and Rabenwald (eastern Alps, Austria). *Econ. Geol.* **84**, 1398-1416.

_____, GAVOILLE, B. & THIÉBAUT, J. (1982): Géochimie des transformations métasomatiques à l'origine du gisement de talc et chlorite de Trimouns (Luzenac, Ariège, France). I. Mobilité des éléments et zonalités. *Bull. Minéral.* **105**, 62-75.

MORIN, G. & BONNIN, D. (1999): Modeling EPR powder spectra using numerical diagonalization of the spin hamiltonian. *J. Magn. Res.* **136**, 176-199.

NOACK, Y., DECARREAU, A. & MANCEAU, A. (1986): Spectroscopic and oxygen isotopic evidence for low and high temperature origin of talc. *Bull. Minéral.* **109**, 253-263.

RABELLO, M.S. & WHITE, J.R. (1996): Photodegradation of talc-filled polypropylene. *Polymer Composites* **17**, 691-704.

RANCOURT, D.G. (1993): Mössbauer spectroscopy of tetrahedral Fe^{3+} in trioctahedral micas. Reply. *Am. Mineral.* **78**, 669-671.

_____ (1994a): Mössbauer spectroscopy of minerals. I. Inadequacy of lorentzian-line doublets in fitting spectra arising from quadrupole splitting distributions. *Phys. Chem. Minerals* **21**, 244-249.

_____ (1994b): Mössbauer spectroscopy of minerals. II. Problem of resolving cis and trans octahedral Fe^{2+} sites. *Phys. Chem. Minerals* **21**, 250-257.

_____, CHRISTIE, I.A.D., ROYER, M., KODAMA, H., ROBERT, J.-L., LALONDE, A.E. & MURAD, E. (1994a): Determination of accurate $^{[4]}Fe^{3+}$, $^{[6]}Fe^{3+}$, and $^{[6]}Fe^{2+}$ site populations in synthetic annite by Mössbauer spectroscopy. *Am. Mineral.* **79**, 51-62.

_____, DANG, M.-Z. & LALONDE, A.E. (1992): Mössbauer spectroscopy of tetrahedral Fe^{3+} in trioctahedral micas. *Am. Mineral.* **77**, 34-43.

_____, MCDONALD, A.M., LALONDE, A.E. & PING, J.Y. (1993): Mössbauer absorber thicknesses for accurate site populations in Fe-bearing minerals. *Am. Mineral.* **78**, 1-7.

_____, PING, J.Y. & BERMAN, R.G. (1994c): Mössbauer spectroscopy of minerals. III. Octahedral-site Fe^{2+} quadrupole splitting distributions in the phlogopite–annite series. *Phys. Chem. Minerals* **21**, 258-267.

RYSAVY, D. & TKADLECKOVA, H. (1992): Surface photooxidation of filled polypropylene. *Polymer Degradation and Stability* **37**, 19-23.

VEDDER, W. (1964): Correlations between infrared spectrum and chemical compositions of micas. *Am. Mineral.* **49**, 736-768.

Received October 30, 1998, revised manuscript accepted July 30, 1999.